



# Chemical component of differences in the endosperm of *Gleditsia* species seeds revealed based on comparative metabolomics

Guanglei Lu, Tingyuan Ren<sup>\*</sup>, Ziyi Zhao, Bei Li, Shuming Tan

College of Liquor and Food Engineering, Guizhou University, Guiyang 55025, China

## ARTICLE INFO

### Keywords:

The endosperm of *Gleditsia* species seeds  
UPLC–ESI–MS/MS  
Network pharmacology approach  
Key active ingredients  
Biomarkers

## ABSTRACT

To investigate the chemical composition and interfunctional differences among the endosperm of *Gleditsia* species seeds (EGS), this study was conducted to determine the metabolic profiles in three EGSs based on the metabolomics approach of UPLC–ESI–MS/MS. A total of 505 metabolites were identified, of which 156 metabolites of EGS were annotated as pharmaceutical ingredients for six human diseases. A total of 110, 146, and 104 metabolites showed different accumulation patterns in the three control groups, LEGS vs. MEGS, LEGS vs. SEGS, and MEGS vs. SEGS, respectively. The metabolic profiles of EGSs differed significantly, and KEGG annotation and enrichment analyses indicated aminoacyl-tRNA biosynthesis as the key metabolic pathway of EGSs. This study enriches the understanding of the chemical composition of EGSs and provides theoretical support for the development and application of EGSs.

## 1. Introduction

The metabolites contained in plants can be categorized into primary metabolites such as amino acids, fatty acids, carbohydrates, and nucleotides and secondary metabolites such as flavonoids, terpenoids, phenylpropanoids, and alkaloids (H. Li et al., 2021). Primary and secondary metabolites of plants not only play an important role in the growth and development of plants but also have nutritional and medicinal values, which are of significance in promoting human health (Hu, Wang, Hu, & Xie, 2020; Wu et al., 2022). For example, flavonoids are widely found in coloured fruits, leaves, and flowers and can precipitate pigments, regulate seed dormancy, and resist biotic and abiotic stresses (Nix, Paull, & Colgrave, 2017). Polyphenols are known to promote gastrointestinal digestion, lower blood pressure, increase body resistance, and work with antioxidants such as vitamin C, vitamin E, and carotenoids to scavenge harmful substances such as free radicals from the body (Musolino et al., 2022). Alkaloids are a class of nitrogenous, alkaline organic compounds found in nature and have a wide range of pharmacological activities, such as anticancer, cardiotoxic, analgesic, and anti-inflammatory activities (Aryal et al., 2022; Ren, Zhang, Wang, Chen, Yang, & Jiang, 2022). The legume (*Leguminosae*) group is the third largest family of flowering plants, is distributed in several climatic zones worldwide and is an important source of food and medicine. The seeds of leguminous plants are rich in flavonoids, alkaloids, phenolic acids and saponins,

which are considered a good source of various nutrients and bioactive metabolites and play important roles in disease prevention and treatment (Farak, Sharaf El-Din, Aboul-Fotouh Selim, Owis, & Abouzid, 2020).

*Gleditsia sinensis* Lam. is a tall deciduous tree that belongs to the *Gleditsia* Linn in the family *Leguminosae* and is widely distributed in areas including East Asia, eastern North America, and South America. The plant is dioecious, with female trees having strong pod-bearing ability and a long fruiting period (Sciarini, Palavecino, Ribotta, & Barrera, 2023). Currently, there are 14 species of *Gleditsia* species in the world, and eight are native to China. Studies have shown that *Gleditsia* species seeds can be used as expectorants and diuretics (Harauchi, Kajimoto, Ohta, Kawachi, Imamura-Jinda, & Ohta, 2017) and have some anti-obesity effects (Lee et al., 2018). The endosperm of *Gleditsia* species seeds (EGS), also known as Zaojiaomi in China, is an important source of galactomannans, which are high in carbohydrates and low in proteins and fats and have high economic and nutritional value (Qin, Liu, Cao, Wang, Ren, & Xia, 2022). The structure of EGS is similar to that of guar gum and acacia carrageenan, which can be used as thickeners, stabilizers, and flocculants (Sun, Li, Wang, Sun, Xu, & Zhang, 2017). Galactomannans derived from EGS, on the other hand, show good functional properties and the potential to alleviate chronic functional bowel diseases and prevent obesity (Takahashi et al., 2009; Thombare, Jha, Mishra, & Siddiqui, 2016) and can be used as a novel phyto-colloid

<sup>\*</sup> Corresponding author.

E-mail address: [tyren@gzu.edu.cn](mailto:tyren@gzu.edu.cn) (T. Ren).

<https://doi.org/10.1016/j.fochx.2023.101060>

Received 9 October 2023; Received in revised form 4 December 2023; Accepted 7 December 2023

Available online 12 December 2023

2590-1575/© 2023 The Author(s). Published by Elsevier Ltd. This is an open access article under the CC BY-NC-ND license (<http://creativecommons.org/licenses/by-nc-nd/4.0/>).

material for food applications (Cerino, Castro, Richard, Exner, & Pensiero, 2018; Loser, Iturriaga, Ribotta, & Barrera, 2021). Meanwhile, *Gleditsia sinensis* semen is listed in the Traditional Chinese Medicine Systems Pharmacology Database and Analysis Platform (TCMSP), which suggests that EGS has good potential for pharmaceutical ingredient mining. However, at present, studies on the metabolic characterization and chemical composition of EGSs are very limited. In addition, different parts of *Gleditsia* species plants (spines, fruits, leaves, seeds, etc.) can be used as sources of different traditional Chinese medicine components and thus have very similar chemical compositions. Therefore, suitable methods are needed to characterize and evaluate the chemical constituents contained in EGSs.

Widely targeted metabolomics has been extensively used in medicine, agronomy, and food as a proven method to assess the value of food with high efficiency, convenience, and accuracy (D. Wang et al., 2018). Network pharmacology is a comprehensive computer method used to establish a “protein compound/disease gene” network to reveal the synergistic therapeutic effects of traditional drugs. It has become a commonly used method in modern drug discovery processes (R. Zhang, Zhu, Bai, & Ning, 2019). Network pharmacology approaches, on the other hand, have been successfully applied in many studies to predict the active ingredients of traditional Chinese medicines and major disease-fighting active pharmaceutical ingredients (Dai et al., 2022; Wang et al., 2020; Zhang et al., 2022). In the present study, the metabolite types and contents in three EGSs were compared using UPLC–ESI–MS/MS in combination with a network pharmacology approach. Thus, the chemical ingredients of EGS were further investigated to provide valuable information for future chemical studies of EGS and the functional development of food products.

## 2. Material and methods

### 2.1. Plant materials

The EGS from *Gleditsia sinensis* Lam. (large endosperm of *Gleditsia* species seeds, LEGS), *G. japonica* var. *delavayi* (medium endosperm of *Gleditsia* species seeds, MEGS), and *Gleditsia japonica* (small endosperm of *Gleditsia* species seeds, SEGS) were provided by Zhijin Zaofu Wanjia Industrial Co., Ltd. (Bijie, China), and three EGS varieties were identified by the institution of Forestry, Guizhou University. Chromatographic purity methanol, acetonitrile, and formic acid were purchased from CNW Technologies (Shanghai, China).

### 2.2. Sample preparation and extraction

The samples were pulverized with a mixer mill at 60 Hz for 240 s. After each sample was accurately weighed, 50 mg of the sample was combined with 700  $\mu$ L of extraction solution (methanol/water = 3:1, cryopreservation at  $-40$  °C, containing the internal standard) and transferred to a centrifuge tube. After vortexing for 30 s, the extract was homogenized at 35 Hz for 4 min and sonicated in an ice-water bath for 5 min, and the homogenization and sonication were repeated three times, followed by overnight extraction on a shaker at 4 °C and centrifugation at 12000 rpm (RCF = 13800 ( $\times$ g), R = 8.6 cm) for 15 min. The supernatant was filtered through a 0.22  $\mu$ m micropore membrane, diluted 10-fold with a methanol/water mixture (v:v = 3:1, containing internal standard), vortexed for 30 s and transferred to 2 mL glass vials, and 100  $\mu$ L of each sample was taken for use in the quality control (QC) cuvette. Samples were stored at  $-80$  °C for UHPLC–MS analysis.

### 2.3. UPLC conditions and ESI-Q TRAP-MS/MS

A UPLC–ESI–MS/MS system (UHPLC, EXION LC system, Shanghai, China; MS, using Sciex QTrap 6500+, Shanghai, China) was used to analyse the substances extracted from EGS samples. The operational parameters and specifications were as follows (Zha, Cai, Yin, Wang, Li,

& Zhu, 2018): mobile phase, eluent A (0.1 % formic acid), eluent B (acetonitrile containing 0.1 % formic acid). An HSS T3 chromatographic column (pore size 1.8  $\mu$ m, length 2.1 mm 100 mm) was used with a column temperature of 40 °C. The temperature of the autosampler was 4 °C, the injection volume was 2  $\mu$ L, and the flow rate was 400  $\mu$ L/min. The analytical gradient program was as follows: the initial conditions were 98 % A, 2 % B, and held for 0.5 min; the linear gradient was converted to 50 % A, 50 % B at 10 min; the linear gradient was converted to 5 % A, 95 % B at 11 min, and held for 2 min; and the linear gradient was adjusted to 98 % A, 2 % B at 13.1 min and held for 2 min. A, 2 % B, and held until 15 min. The effluent was delivered to the ESI-Q-TRAP-MS system.

Linear ion trap (LIT) and triple quadrupole (QQQ) scans were obtained on a 6500 QTrap UPLC/MS/MS system coupled with an ESI Turbo Ion Spray interface operating in positive and negative ionization modes and processed by Analyst 1.6.3 software (AB Sciex). Mass spectrometry and ESI source conditions were as described previously (Shi et al., 2019): ion source, Turbo Spray; source temperature, 400 °C; ion spray voltage (IS), +5500 (positive ionization mode)/ $-4500$  V (negative ionization mode); ion source gas I (GSI), gas II (GS II), and curtain gas (CUR) of 60, 30, and 35 psi, respectively; and collision gas, high. Instruments were tuned and quality calibrated with 10  $\mu$ mol/L and 100  $\mu$ mol/L polypropylene glycol solutions in QQQ and LIT modes. QQQ scans were obtained as multiple reaction monitoring (MRM) experiments. The clustering potential (DP) and collision energy (CE) were optimized for individual MRM jumps. A specific set of MRM transitions was monitored for each period based on the elution of metabolites during this period.

### 2.4. Qualitative and quantitative metabolites analysis

A combination of self-built software databases and public metabolite databases (MassBank, HMDB, ChemBank, PubChem, and METLIN) was used to qualitatively annotate metabolites in EGS using primary and secondary MS data (Cao et al., 2022; Z.-M. Zhang et al., 2015). After eliminating initial interferences from nontarget ions, fragment ion information with desired characteristics was obtained by QQQ. After obtaining the basic mass spectrometry data of the metabolites, the relative amount of each metabolite in different samples was determined by the chromatographic peak area; the mass spectrometry data were integrated and corrected using MultiaQuant software.

The Z score-normalized metabolic data of all EGS and QC samples were subjected to multivariate statistical analyses, including principal component analysis (PCA), hierarchical clustering analysis (HCA), and orthogonal partial least squares-discriminant analysis (OPLS-DA), using R software. Differentially abundant metabolites were screened during two-by-two comparisons, and OPLS-DA was performed using log<sub>2</sub>-transformed metabolic data, with the criteria set at a P value < 0.05 for Student's *t*-test (STT) and a threshold variable importance projection (VIP) > 1. OPLS-DA was verified by 200 alignment model stability, and finally, the Kyoto Encyclopedia of Genes and Genomes (KEGG, <https://www.kegg.jp/kegg/>) was used for labelling and enrichment analysis of differentially abundant metabolites.

### 2.5. Identification of key herbal active ingredients in EGS

The metabolites identified from EGS by the UPLC–ESI–MS/MS system were further queried in TCMSP (version 2.3, <https://old.tcmssp-e.com/tcmssp.php>). Metabolites were considered key active ingredients belonging to EGS in TCMSP when they had oral bioavailability (OB)  $\geq 5$  % and drug-likeness (DL)  $\geq 0.14$  (Xia et al., 2023). Relevant targets and diseases were included in the TCMSP database annotations.

### 2.6. Identification of anti-human disease drug components in EGS

First, all identified metabolites were queried in the CancerHSP

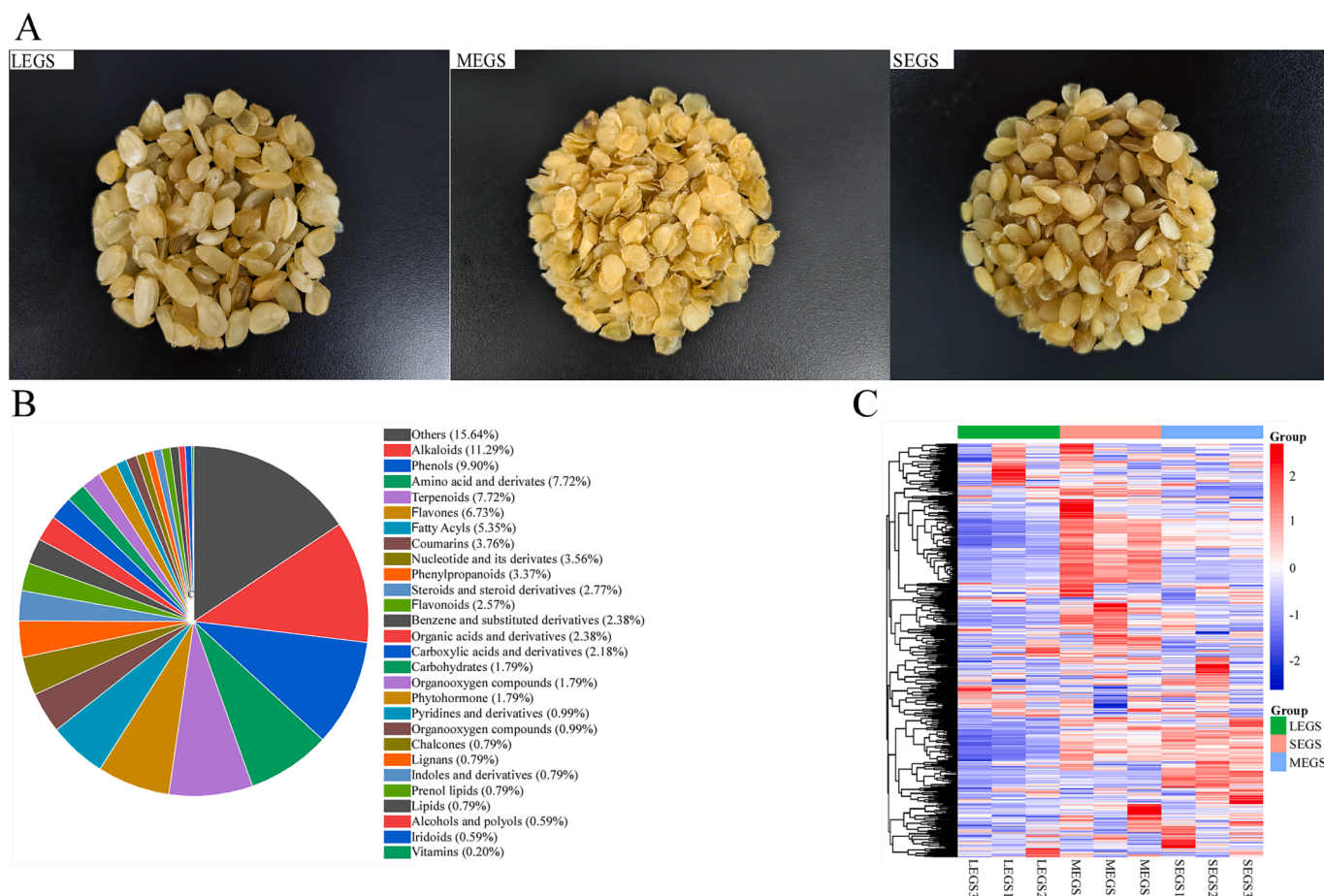


**Fig. 1.** Analysis and identification of metabolites in EGS. **A:** Pictures of LEGS, MEGS, and SEGS from left to right. **B:** Compositional analysis of metabolites. The types, amounts, and proportions of all identified metabolites are shown above. **C:** HCA analysis of three EGS metabolites. Each sample is represented by a column and each metabolite is shown in a row. Red represents high level and blue represents low level. (For interpretation of the references to colour in this figure legend, the reader is referred to the web version of this article.)

database in the TCMSP analysis platform (Ru et al., 2014) to detect anticancer/tumour components. Second, five disease names, “Alzheimer’s disease”, “analgesics”, “inflammation”, “pain (unspecified)”, and “arthritis”, were individually inputted in the disease name menu under the TCMSP database to search for ingredients related to resistance to each of the diseases. Finally, the metabolites identified by UPLC–ESI–MS/MS analysis were compared with the anti-disease-related components obtained to identify the effective drug components against diseases in EGS.

### 2.7. Statistical analysis

Comparisons of relative levels of EGS differentially abundant metabolites were performed using Duan multiple comparisons in IBM SPSS Statistics (version 28).

## 3. Results and discussion

### 3.1. Identification of EGS metabolites

In this study, the composition of relevant metabolites in three different species (three replicates per sample) of EGS was determined by UPLC–ESI–MS/MS widely targeted metabolomics. Total ion current (TIC) analysis of QC samples was used to check the consistency of the metabolite extraction and assay. The TIC curves and metabolite assay results overlapped (Fig. S1A and B). When the same sample was identified at different times, the retention time and peak intensity remained

constant, indicating signal stability (R2 close to 1, Fig. S1C). After quality assessment, 505 metabolites were initially identified, which could be classified into 28 categories, including 57 alkaloids, 50 phenols, 39 amino acids and derivatives, 39 terpenoids, 34 flavones, 27 fatty acyls, 19 coumarins, 18 nucleotides and derivatives, 11 phenylpropanoids, 79 others, etc., and detailed information of all metabolite identifiers is shown in Table S1. The nine samples could be divided into three groups by assessing the clustered heatmap (Fig. 1C), and the relative contents of MEGS metabolites were significantly different than those of LEGS and SEGS, indicating that there was a significant disparity in metabolites among the three EGSs that were affected by genetic variation.

### 3.2. Screening of key active herbal components in EGS

There is a lack of research on the nutritional value and functional attributes of EGS, which greatly limits its potential application as a food. Therefore, further screening of active ingredients related to traditional Chinese medicine based on EGS metabolites can help to reveal the chemical basis of EGS-related health functions and their potential value. Based on this, we conducted a query in the TCMSP database for active ingredients in EGS that can promote human health. The results showed that among 505 metabolites identified, a total of 221 were found to be chemical components of traditional Chinese medicine in the TCMSP. According to the screening criteria of OB  $\geq 5\%$  and DL  $\geq 0.14$ , 93 of the 221 metabolites detected were found to be key active ingredients used in TCMSP. In particular, 40 of these 93 metabolites met the screening

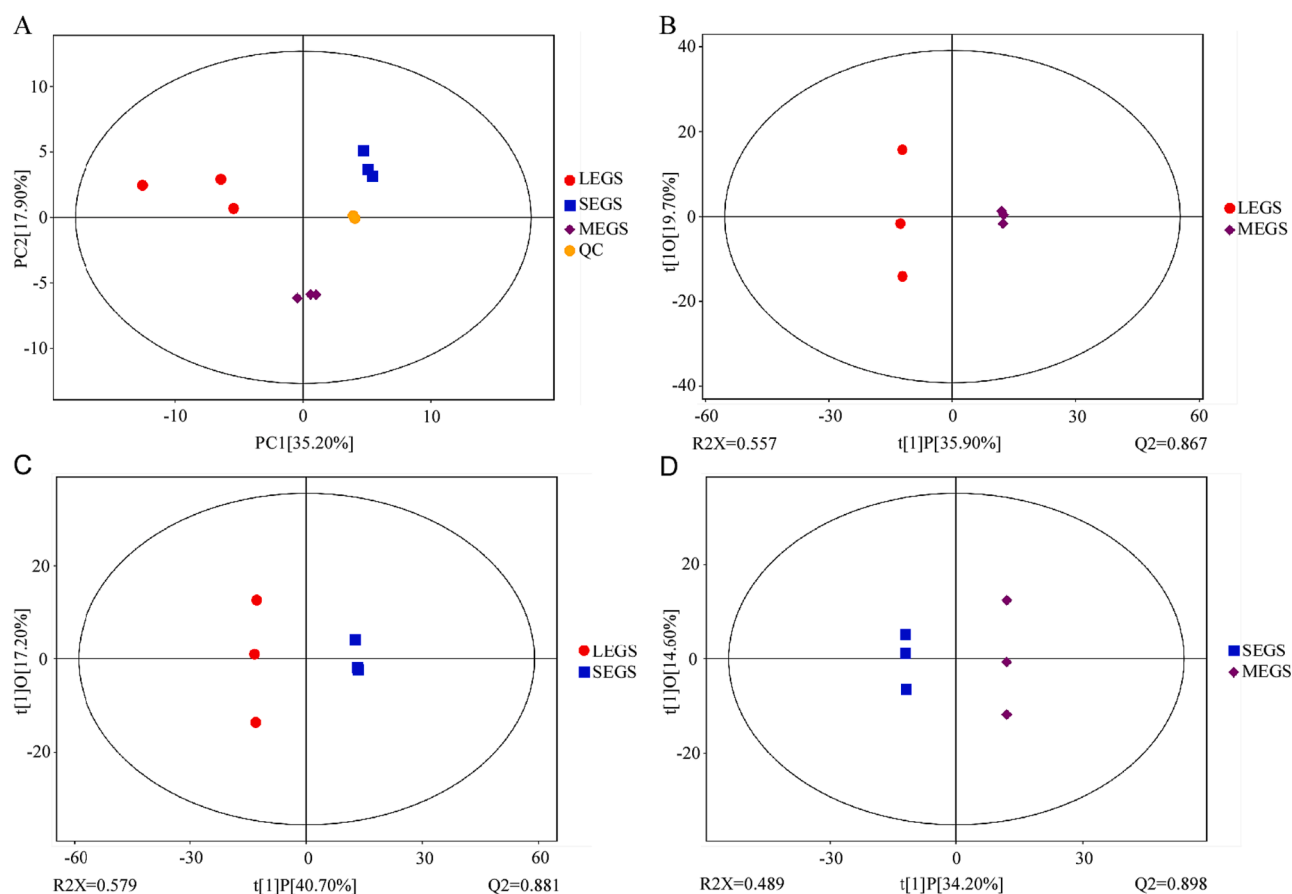


**Fig. 2.** PCA and OPLS-DA analyses of the three EGSs. A: Plot of PCA scores for LEGS, MEGS, SEGS, and QC; different colour represent different groups: red = LEGS sample; purple = MEGS sample; blue = SEGS sample; and orange = QC sample; the horizontal and vertical coordinates denote the first and the second principal components PC1 and PC2, respectively. B, C and D are plots of OPLS-DA model scores for LEGS vs. MEGS, LEGS vs. SEGS, and SEGS vs. MEGS, respectively. (For interpretation of the references to colour in this figure legend, the reader is referred to the web version of this article.)

criteria for potential drug candidates ( $OB \geq 30\%$ ,  $DL \geq 0.18$ ), and these 40 metabolites belonged to the core key active ingredients in TCMS (Table S2). These 93 key active ingredients included 23 flavonoids, 17 terpenoids, 8 phenols, 8 steroids and steroid derivatives, 6 alkaloids, 6 coumarins, 6 fatty acyls, 4 nucleotides and derivatives, 2 lignans, 1 phenylpropanoid, 1 carbohydrate, 1 organooxygen compound, 1 lipid, and 9 others; 40 core key active ingredients included 10 terpenoids, 9 flavonoids, 8 steroids and their derivatives, 4 coumarins, 2 phenols, 2 fatty acyls, 1 lignin, 1 nucleotide and its derivative, and 3 others (Table S2). The results showed that EGS is rich in key active ingredients that can promote human health. Among these active ingredients, flavonoids and terpenoids are the main active substances exerting health effects in EGS, while other types of metabolites, such as steroids and their derivatives, phenols, alkaloids, coumarins, and fatty acyls, also have important health-promoting effects. Among these 93 key components, 68 metabolites were associated with 249 target proteins and corresponded to 304 diseases. Meanwhile, 40 metabolites that met the screening criteria for potential drugs were associated with 160 target proteins and 263 diseases (Ru et al., 2014). These diseases mainly include cancer/tumour, Alzheimer's disease, analgesics, inflammation, pain (unspecified), and arthritis. The results suggest that these screened metabolites are key or core active components of EGS that are relevant to human health. In addition, 25 metabolites did not have corresponding target proteins and diseases, but nine metabolites had very high DL values ( $DL \geq 0.65$ ), especially cycloeucaenol, ganoderic acid F, rhoifolin, dipterocarpol, talatisamine, ganoderol A, taraxerol, and seven metabolites had extremely high DL values ( $DL \geq 0.72$ ), including the flavanoid rhoifolin, the alkaloid talatisamine, and five terpenoid

metabolites (Table S2). These nine metabolites have important human health-promoting effects and have good potential for novel drug development.

### 3.3. Screening of active pharmaceutical ingredients for six human diseases in EGS

Six diseases identified in the screen, namely, cancer/tumour, Alzheimer's disease, analgesics, inflammation, pain (unspecified), and arthritis, pose serious threats to human health. Based on the above key active ingredient labelling results, these six diseases are also the main diseases associated with the metabolites of the core key active substances in EGS. However, whether the key active ingredients identified above are also active pharmaceutical ingredients against these six diseases needs to be further analysed.

To further identify the key disease-resistant components in EGS that are active against these six diseases, we queried the TCMS database for 505 metabolites identified in EGS (Ru et al., 2014). The results showed that a total of 156 metabolites corresponding to at least one disease were identified in the three EGSs. These 156 metabolites included 27 flavonoids, 22 amino acids and derivatives, 16 phenols, 10 terpenoids, 9 phytohormones, 7 alkaloids, 6 phenylpropanoids, 6 carbohydrates, 6 steroids and steroid derivatives, 5 coumarins, 5 fatty acyls, 4 organooxygen compounds, 3 organic acids and derivatives, 2 alcohols and polyols, 2 lipids, 1 benzene and substituted derivative, 1 carboxylic acid and its derivative, 1 lignan, 1 nucleotide and its derivative, and 22 others (Table S3). Among them, there were 47, 56, 54, 126, 54, and 54 metabolites corresponding to cancer/tumour, Alzheimer's disease,

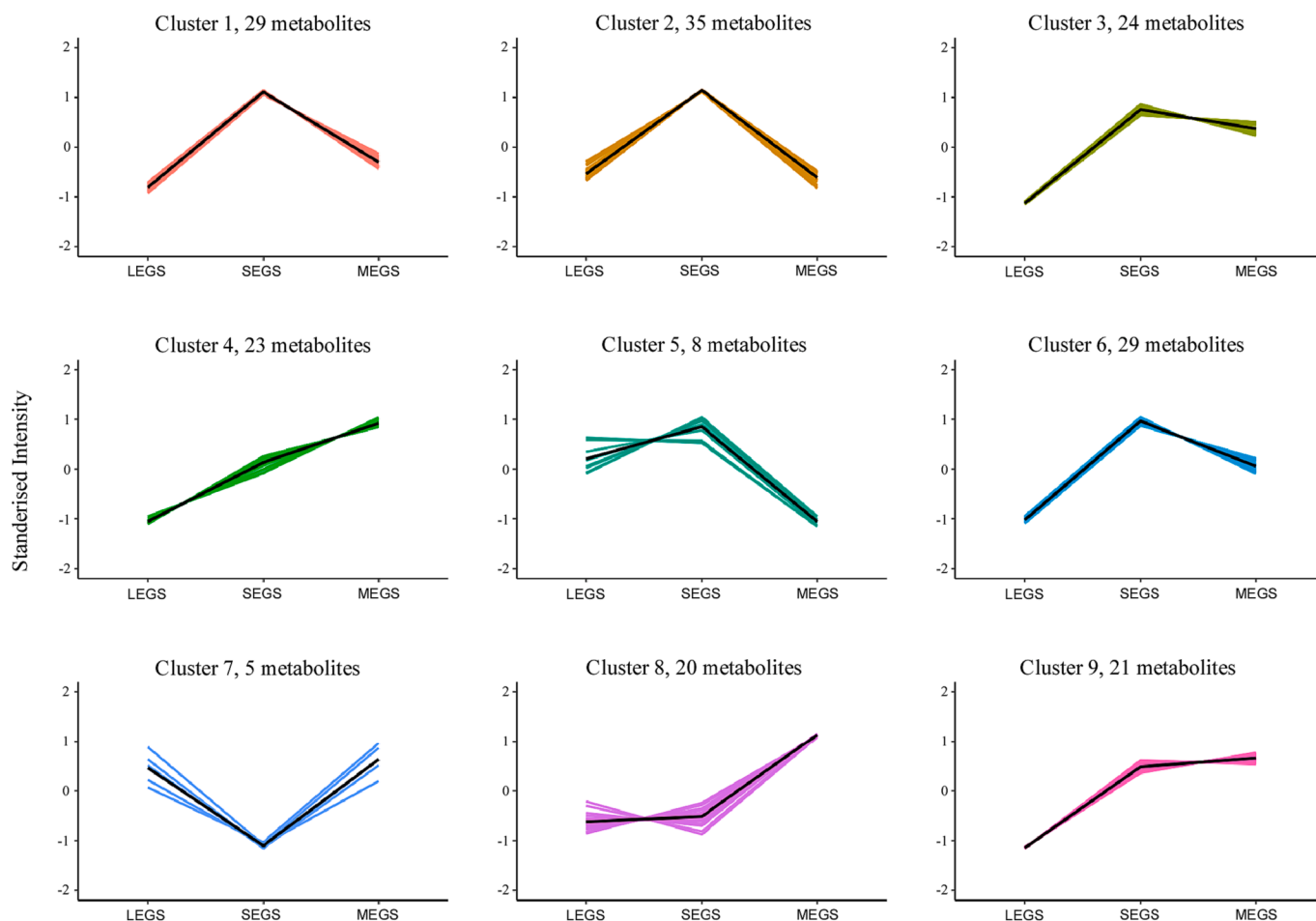


**Fig. 3.** K-means clusters of the expression profiles of the three EGS differentially abundant metabolites. The y-axis represents the normalized metabolite content and the x-axis represents the different samples.

analgesics, inflammation, pain (unspecified), and arthritis, respectively. Notably, some metabolites confer resistance to multiple diseases; for example, 16 metabolites, such as apigenin, confer resistance to all six of these diseases, 35 metabolites, such as arachidonic acid, confer resistance to five diseases, curcuminol confers resistance to four diseases, ellagic acid and isopulegol confer resistance to three diseases, and 7 metabolites, such as biochanin A, confer resistance to 2 diseases (Table S3). These 156 metabolites also contained 55 active substances of TCMS described above, suggesting that these metabolites may be the most critical active pharmaceutical ingredients in EGS that function to protect against the six human diseases mentioned above. However, the specific efficacy of these metabolites must be further verified.

### 3.4. PCA and OPLS-DA of three EGSs

PCA achieves the goal of analysing the internal structure of numerous variables using a small number of principal components (Qian et al., 2023). In the PCA score plot, the cumulative contribution of the two principal components (PC1 35.20 % × PC2 17.90 %) amounted to 53.10 %. As shown in Fig. 2A, LEGS, MEGS, and SEGS could be easily separated, indicating that the metabolites of the three varieties of EGS differed significantly and that the three biological replicates of each variety formed a tight cluster. The experimental results showed that the sample material was sufficiently reproducible and suitable for subsequent qualitative and quantitative analyses Fig. 3.

In this study, all metabolites of EGSs were evaluated using a two-by-two comparison method based on the OPLS-DA model to determine the differences between LEGS and MEGS ( $Q^2 = 0.867$ ,  $R^2 X = 0.557$ ,  $R^2 Y$

$= 1$ ; Fig. 2B), LEGS and SEGS ( $Q^2 = 0.881$ ,  $R^2 X = 0.579$ ,  $R^2 Y = 1$ ; Fig. 2C), and MEGS and SEGS ( $Q^2 = 0.898$ ,  $R^2 X = 0.489$ ,  $R^2 Y = 1$ ; Fig. 2D). The colours and shapes of the scattered dots indicate different groupings; The closer the distribution of sample dots, the more similar the types and levels of metabolites in the samples; Conversely, the further away the samples, the greater the differences in their overall metabolic levels. The samples were all within the 95 % confidence interval. The overall distribution trend of the samples can be reflected by looking at the PCA score plots of all the samples. This shows that these models are reliable and stable and can better explain the metabolic changes of the three varieties, which can be used for further screening of metabolites using VIP analysis. The OPLS-DA score plots showed that the EGS of the three varieties were separated, which indicated that the metabolic phenotypes of the three varieties differed significantly.

### 3.5. Screening and analysis of key differentially abundant metabolites of the three EGSs

In this study, we compared LEGS vs. MEGS, LEGS vs. MEGS, and MEGS vs. SEGS using  $P$  value  $< 0.05$  and  $VIP > 1$  as the screening conditions and identified the most meaningful differentially abundant metabolites from 505 metabolites. There were a total of 110 differentially abundant metabolites between the LEGS and MEGS groups (1 upregulated and 109 downregulated, Fig. S2A), 146 differentially abundant metabolites between the LEGS and SEGS groups (2 upregulated and 144 downregulated, Fig. S2B), and 104 differentially abundant metabolites between the MEGS and SEGS groups (31 upregulated and 73 downregulated, Fig. S2C). The differentially abundant metabolites in the

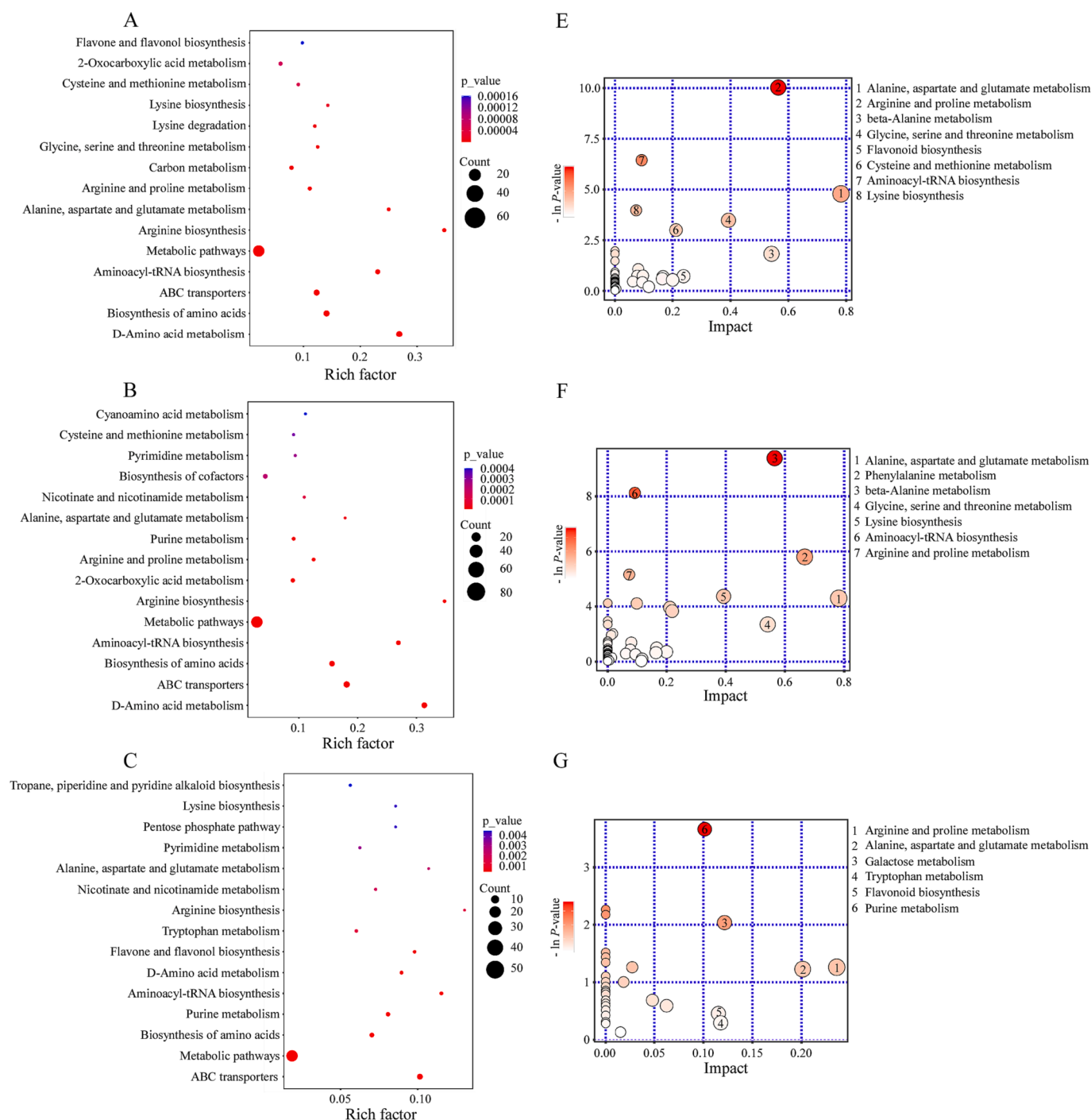


**Fig. 4.** KEGG pathway enrichment analysis of three groups of EGS. A-C: KEGG enrichment pathways of differentially accumulated metabolites among groups (LEGS vs. MEGS, LEGS vs. SEGS, MEGS vs. SEGS); E-G: differentially accumulated metabolites among groups (LEGS vs. MEGS, LEGS vs. SEGS, MEGS vs. SEGS) of the HMDB, PubChem, and KEGG co-enrichment pathways.

three control groups could be categorized into 24 (LEGS vs. SEGS group), 21 (LEGS vs. MEGS group), and 22 (MEGS vs. SEGS group) different categories. Among them, the most significantly upregulated metabolite in the LEGS vs. MEGS group was 3-ethoxy-4-hydroxybenzaldehyde, and the most significantly downregulated was meloside A (Fig. S2D); The most significantly upregulated metabolite in the LEGS vs. SEGS group was L-homocitrulline, and the most significantly downregulated was L-isoleucine (Fig. S2E); the most significantly upregulated metabolite in the MEGS vs. SEGS group was kynurenic acid, and the most significantly downregulated metabolite was N1-methyl-2-pyridone-5-carboxamide (Fig. S2F). The total number of differentially

abundant metabolites in the three EGSs was 29, including 10 amino acids and derivatives, three alkaloids, two flavonoids, two fatty acyls, two phytohormones, one phenol, one indole and derivative, one organic acid and derivative, one nucleotide and its derivative, one flavonoid, one carboxylic acid and derivative, one aromatic compound, and three others. These 29 differentially abundant metabolites may be potential biomarkers for EGS.

In addition, the highest percentage of differentially abundant metabolites in the LEGS vs. SEGS group, LEGS vs. MEGS group, and MEGS vs. SEGS group were amino acids and derivatives, which accounted for 19.80 %, 24.70 %, and 14.50 %, respectively, and the distribution of

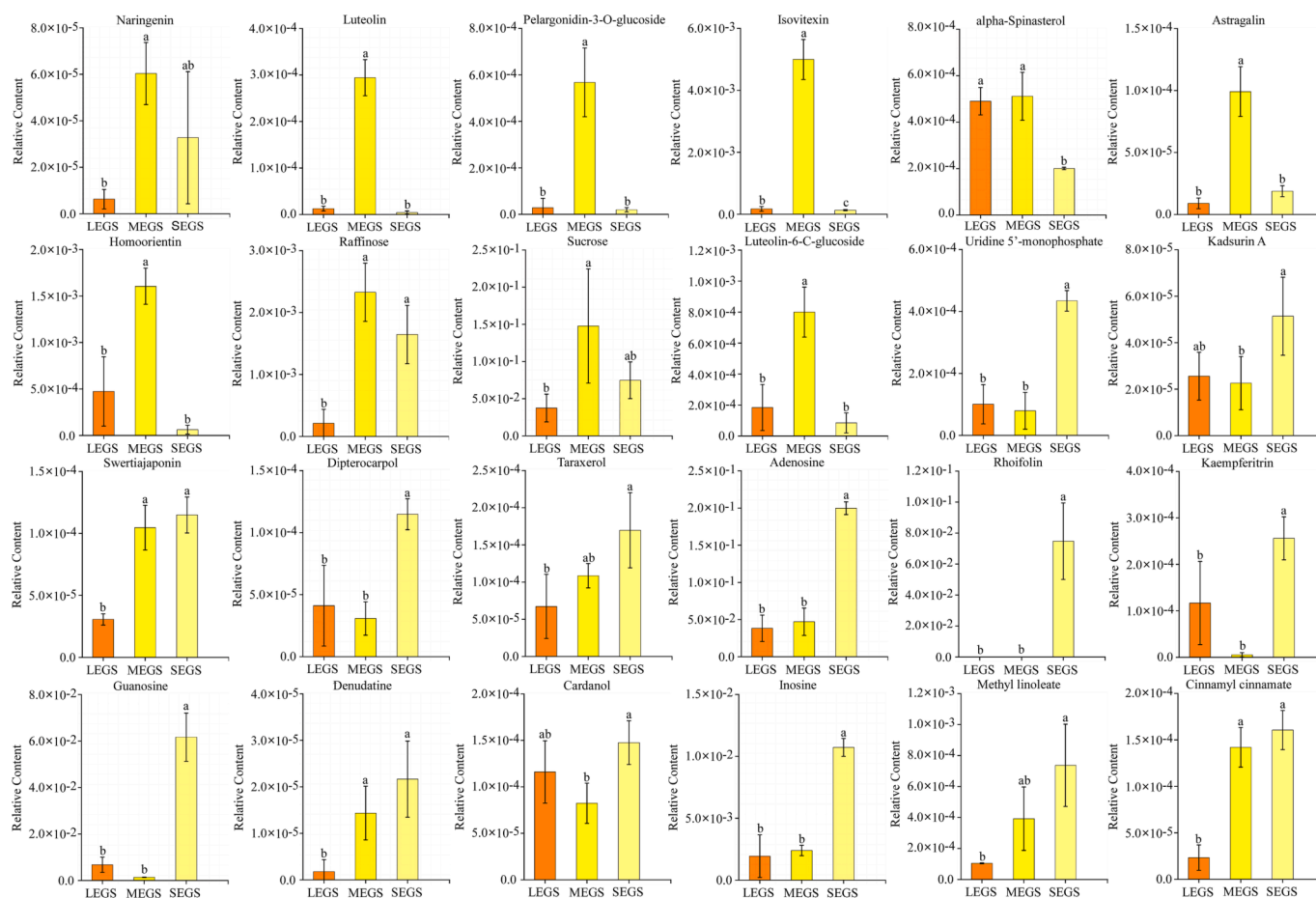


**Fig. 5.** Comparison of the relative contents of 24 key active ingredients of the three EGS in TCMSP. Each relative content is the mean ( $\pm$ SD) of the relative contents of the three EGS differentially abundant metabolites.

nucleotides and their derivatives, flavonoids, alkaloids, and phenols also significantly differed among the three groups. To further analyse EGS metabolites, we classified 194 differentially abundant metabolites into nine subclasses based on the K-means method as a way to study the trends of the relative contents of metabolites in different subgroups. Among these subclasses, subclass 1, subclass 2, subclass 3, subclass 5, and subclass 6 all showed higher differentially abundant metabolite contents in SEGS than in LEGS and MEGS, while subclass 7 showed the opposite trend, and subclasses 4, 8, and 9, had the highest differentially abundant metabolite contents in MEGS. The results showed that the SEGS had a higher relative content of metabolites than the other two EGSs, despite being smaller than the other two in appearance and morphology. In addition, a total of 22 TCM active ingredients were found in the differentially abundant metabolites of LEGS vs. SEGS, LEGS vs. MEGS, and MEGS vs. SEGS, including uridine 5'-monophosphate, swertiajaponin, alpha-spinasterol, naringenin, luteolin, and pelargonidin-3-O-glucoside. These six differentially abundant metabolites are key active ingredients and core pharmaceutical active ingredients of TCMSP that were retrieved in TCMSP.

### 3.6. KEGG analysis of EGS

The KEGG metabolic pathway database is a powerful tool for metabolic analysis and metabolic network studies that graphically illustrates various cellular synthesis and degradation processes (S. Li et al., 2018). Therefore, KEGG can be used to enrich and analyse differentially abundant metabolites in samples of differently coloured particles to obtain comprehensive functional information. Differentially abundant metabolites in the LEGS vs. MEGS group, LEGS vs. SEGS group, and

MEGS vs. SEGS group were involved in 51, 57, and 39 pathways, respectively. The first 15 metabolic pathways in the three control groups were mainly associated with “metabolic pathways, biosynthesis of secondary metabolites”, “D-amino acid metabolism”, “biosynthesis of amino acids”, “ABC transporters”, “aminoacyl-tRNA biosynthesis”, and “biosynthesis of cofactors” (Fig. 4A – C). To find the key pathways with the highest correlation with metabolite differences, we further analysed the pathways of differentially abundant metabolites. The results showed that 41, 47, and 31 metabolic pathways were enriched in the LEGS vs. MEGS group, LEGS vs. SEGS group, and MEGS vs. SEGS group, respectively, 24 metabolic pathways were enriched in all three groups, and differentially abundant metabolites were most significantly enriched in the “aminoacyl-tRNA biosynthesis pathway”, followed by “arginine and proline metabolism” (Fig. 4D – F). These results suggest that “aminoacyl-tRNA biosynthesis” is a key metabolic pathway for all three EGSs.

### 3.7. Analysis of biomarkers of the three EGSs

Flavonoids are an important class of plant metabolites, including flavones, flavonoids, flavanols, and chalcones. Many reports have shown that flavonoids can prevent diseases such as cardiovascular disease, cancer, and inflammation due to their antioxidant activity (Nie et al., 2020). Based on the above results, the metabolic phenotypes and differentially abundant metabolites of the three EGSs were different because they were derived from different *Gleditsia*. To further understand the nutritional and functional values among the three EGSs, we comparatively analysed the relative contents of metabolites belonging to the key active ingredients in TCMSP among the three EGSs.

Based on these results, we screened a total of 24 compounds with

significant differences in relative content from 93 metabolites that met the screening criteria for key active ingredients in TCMSp. These 24 metabolites included 10 flavonoids, 4 nucleotides and their derivatives, 2 terpenoids, 1 phenylpropanoid, 1 phenol, 1 lignan, 1 alkaloid, 1 carbohydrate, 1 organooxygen compound, 1 steroid and steroid derivative, and 1 other metabolite with the highest proportion of flavonoids (41.67 %, Table S2). Among these 24 metabolites, 10 had the highest relative content in the MEGS, and the remaining 12 had the highest relative content in the SEGS. In particular, seven flavonoids, naringenin, luteolin, pelargonidin-3-O-glucoside, isovitexin, astragalol, homoorientin, and luteolin-6-C-glucoside, had the highest relative content in the MEGS. Swertiajaponin, rhoifolin, and kaempferitrin were the three species with the highest relative contents in the SEGS (Fig. 5). In terms of origin, the LEGS and SEGS were both double-pod EGSs, mainly produced in Guizhou, China, while the MEGS was a single-pod EGS, mainly produced in Yunnan, China, and the difference in the growth environment greatly affected the quality of the EGS. The relative content of flavonoids in the MEGS produced in Yunnan, China was the highest, while the content of flavonoids in the SEGS, which is also a two-pod EGS but smaller in size, was instead higher than that in the LEGS, so the size of the EGS was not positively correlated with the relative content of its metabolites. In addition, in combination with the above results (Fig. 2), the relative contents of SEGS were higher than those of MEGS in a variety of metabolites. Based on 24 different metabolites, we can obtain a clearer understanding of the differences in the chemical composition of the three EGSs.

#### 4. Conclusion

In this study, the differences in 505 metabolites in the metabolic profiles of the three EGSs were systematically evaluated using the UPLC-ESI-MS/MS metabolomics approach. Among these 505 metabolites, 156 active ingredients of metabolites targeting six anti-diseases in humans were annotated by network pharmacology methods. PCA and OPLS-DA analyses revealed significant differences in the metabolic phenotypes of the three EGSs and in the three comparison groups: LEGS vs. MEGS, LEGS vs. SEGS, and MEGS vs. SEGS. There were 110, 146, and 104 differentially abundant metabolites and a total of 29 differentially abundant metabolites in the three groups, respectively. K-means clustering analysis showed that SEGS had a higher level of multiple metabolites than LEGS and MEGS. KEGG annotation and enrichment results indicated that the aminoacyl-tRNA biosynthesis pathway was the key pathway for the synthesis of EGS metabolites. In addition, a total of 24 metabolites with significant relative content differences were screened from the key active ingredients in TCMSp, among which flavonoids accounted for the largest proportion, and the relative contents of several flavonoids in the MEGS were higher than those in the LEGS and SEGS. The present study provides useful information on the chemical composition and basis of EGSs with health-promoting functions, which is important for understanding the nutritional and functional properties of EGSs.

#### CRedit authorship contribution statement

**Guanglei Lu:** Investigation, Methodology, Formal analysis, Writing – original draft. **Tingyuan Ren:** Supervision, Investigation, Writing – review & editing, Funding acquisition. **Ziyi Zhao:** Investigation, Validation. **Bei Li:** Investigation, Validation. **Shuming Tan:** Conceptualization, Supervision.

#### Declaration of competing interest

The authors declare that they have no known competing financial interests or personal relationships that could have appeared to influence the work reported in this paper.

#### Data availability

No data was used for the research described in the article.

#### Funding

This research has been supported by the China National Key R&D Program (Grant No. 2022YFD1601712).

#### Appendix A. Supplementary data

Supplementary data to this article can be found online at <https://doi.org/10.1016/j.fochx.2023.101060>.

#### References

- Aryal, B., Raut, B. K., Bhattarai, S., Bhandari, S., Tandan, P., Gyawali, K., ... Parajuli, N. (2022). Potential Therapeutic Applications of Plant-Derived Alkaloids against Inflammatory and Neurodegenerative Diseases. *Evidence-based Complementary and Alternative Medicine*, 2022, 7299778. <https://doi.org/10.1155/2022/7299778>
- Cao, K., Wang, B., Fang, W., Zhu, G., Chen, C., Wang, X., ... Wang, L. (2022). Combined nature and human selections reshaped peach fruit metabolome. *Genome Biology*, 23 (1), 146. <https://doi.org/10.1186/s13059-022-02719-6>
- Cerino, M. C., Castro, D. C., Richard, G. A., Exner, E. d. L., & Pensiero, J. F. (2018). Functional dioecy in *Gleditsia* amorphoides (Fabaceae). *Australian Journal of Botany*, 66(1), 85. <https://doi.org/10.1071/bt16185>
- Dai, Y., Zhang, K., Wang, L., Xiong, L., Huang, F., Huang, Q., ... Zeng, J. (2022). Rapid Profiling of Metabolites Combined with Network Pharmacology to Explore the Potential Mechanism of *Sanguisorba officinalis* L. against Thrombocytopenia. *Metabolites*, 12(11), 1074. <https://doi.org/10.3390/metabo12111074>
- Farag, M. A., Sharaf El-Din, M. G., Aboul-Fotouh Selim, M., Owis, A. I., & Abouzid, S. F. (2020). Mass Spectrometry Profiling of Nutrients and Anti-Nutrients in Major Legume Sprouts. *Food Bioscience*, 100800. <https://doi.org/10.1016/j.fbio.2020.100800>
- Harauchi, Y., Kajimoto, T., Ohta, E., Kawachi, H., Imamura-Jinda, A., & Ohta, S. (2017). Prenylated purine alkaloids from seeds of *Gleditsia japonica*. *Phytochemistry*, 143, 145–150. <https://doi.org/10.1016/j.phytochem.2017.08.006>
- Hu, H., Wang, J., Hu, Y., & Xie, J. (2020). Nutritional component changes in Xiangfen 1 banana at different developmental stages. *Food & Function*, 11(9), 8289–8296. <https://doi.org/10.1039/d0fo00999g>
- Lee, J.-H., Go, Y., Lee, B., Hwang, Y.-H., Park, K. I., Cho, W.-K., & Ma, J. Y. (2018). The fruits of *Gleditsia sinensis* Lam. inhibits adipogenesis through modulation of mitotic clonal expansion and STAT3 activation in 3T3-L1 cells. *Journal of Ethnopharmacology*, 61. <https://doi.org/10.1016/j.jep.2018.04.020>
- Li, H., Lv, Q., Liu, A., Wang, J., Sun, X., Deng, J., ... Wu, Q. (2021). Comparative metabolomics study of Tartary (*Fagopyrum tataricum* (L.) Gaertn) and common (*Fagopyrum esculentum* Moench) buckwheat seeds. *Food Chemistry*, 371, Article 131125. <https://doi.org/10.1016/j.foodchem.2021.131125>
- Li, S., Dong, X., Fan, G., Yang, Q., Shi, J., Wei, W., ... Zhao, Z. (2018). Comprehensive Profiling and Inheritance Patterns of Metabolites in Foxtail Millet. *Frontiers in Plant Science*, 9. <https://doi.org/10.3389/fpls.2018.01716>
- Loser, U., Iturrriaga, L., Ribotta, P. D., & Barrera, G. N. (2021). Combined systems of starch and *Gleditsia triacanthos* galactomannans: Thermal and gelling properties. *Food Hydrocolloids*, 112, Article 106378. <https://doi.org/10.1016/j.foodhyd.2020.106378>
- Musolino, V., Macri, R., Cardamone, A., Serra, M., Coppoletta, A. R., Tucci, L., ... Mollace, V. (2022). Nocellara Del Belice (*Olea europaea* L. Cultivar): Leaf Extract Concentrated in Phenolic Compounds and Its Anti-Inflammatory and Radical Scavenging Activity. *Plants*, 12, 27. <https://doi.org/10.3390/plants12010027>
- Nie, H., Chen, H., Li, G., Su, K., Song, M., Duan, Z., ... Luo, Y. (2020). Comparison of flavonoids and phenylpropanoids compounds in Chinese water chestnut processed with different methods. *Food Chemistry*, 335, Article 127662. <https://doi.org/10.1016/j.foodchem.2020.127662>
- Nix, A., Paull, C., & Colgrave, M. (2017). Flavonoid Profile of the Cotton Plant. *Gossypium hirsutum: A Review*. *Plants*, 6, 43. <https://doi.org/10.3390/plants6040043>
- Qian, G., Li, X., Zhang, H., Zhang, H., Zhou, J., Ma, X., ... Li, L. (2023). Metabolomics analysis reveals the accumulation patterns of flavonoids and phenolic acids in quinoa (*Chenopodium quinoa* Willd.) grains of different colors. *Food Chemistry: X*, 17, 100594. doi: 10.1016/j.fochx.2023.100594.
- Qin, N., Liu, H., Cao, Y., Wang, Z., Ren, X., & Xia, X. (2022). Polysaccharides from the seeds of *Gleditsia sinensis* Lam. attenuate DSS-induced colitis in mice via improving gut barrier homeostasis and alleviating gut microbiota dysbiosis. *Food & Function*, 14, 122–132. <https://doi.org/10.1039/d2fo02722d>
- Ren, Z., Zhang, H., Wang, Z., Chen, X., Yang, L., & Jiang, H. (2022). Progress in Immunoassays of Toxic Alkaloids in Plant-Derived Medicines: A Review. *Toxins*, 14, 165. <https://doi.org/10.3390/toxins14030165>
- Ru, J., Li, P., Wang, J., Zhou, W., Li, B., Huang, C., ... Yang, L. (2014). TCMSp: A database of systems pharmacology for drug discovery from herbal medicines. *Journal of Cheminformatics*, 6(1). <https://doi.org/10.1186/1758-2946-6-13>



- Sciarini, L. S., Palavecino, P. M., Ribotta, P. D., & Barrera, G. N. (2023). Gleditsia triacanthos Galactomannans in Gluten-Free Formulation: Batter Rheology and Bread Quality. *Foods*, *12*, 756. <https://doi.org/10.3390/foods12040756>
- Shi, X., Wang, S., Jasbi, P., Turner, C., Hrovat, J., Wei, Y., ... Gu, H. (2019). Database-Assisted Globally Optimized Targeted Mass Spectrometry (dGOT-MS): Broad and Reliable Metabolomics Analysis with Enhanced Identification. *Analytical Chemistry*, *91*, 13737–13745. <https://doi.org/10.1021/acs.analchem.9b03107>
- Sun, M., Li, Y., Wang, T., Sun, Y., Xu, X., & Zhang, Z. (2017). Isolation, fine structure and morphology studies of galactomannan from endosperm of Gleditsia japonica var. delavayi. *Carbohydrate Polymers*, *184*. <https://doi.org/10.1016/j.carbpol.2017.12.003>
- Takahashi, T., Yokawa, T., Ishihara, N., Okubo, T., Chu, D.-C., Nishigaki, E., ... Raj Juneja, L. (2009). Hydrolyzed guar gum decreases postprandial blood glucose and glucose absorption in the rat small intestine. *Nutrition Research*, *29*(6), 419–425. <https://doi.org/10.1016/j.nutres.2009.05.013>
- Thombare, N., Jha, U., Mishra, S., & Siddiqui, M. Z. (2016). Guar gum as a promising starting material for diverse applications: A review. *International Journal of Biological Macromolecules*, *88*, 361–372. <https://doi.org/10.1016/j.ijbiomac.2016.04.001>
- Wang, D., Zhang, L., Huang, X., Wang, X., Yang, R., Mao, J., ... Li, P. (2018). Identification of Nutritional Components in Black Sesame Determined by Widely Targeted Metabolomics and Traditional Chinese Medicines. *Molecules*, *23*, 1180. <https://doi.org/10.3390/molecules23051180>
- Wang, L., Li, H., Shen, X., Zeng, J., Yue, L., Lin, J., ... Wu, J. (2020). Elucidation of the molecular mechanism of Sanguisorba officinalis L. against leukopenia based on network pharmacology. *Biomedicine & Pharmacotherapy*, *132*. <https://doi.org/10.1016/j.biopha.2020.110934>
- Wu, Y., Huang, X., Yang, H., Zhang, S., Lyu, L., Li, W., & Wu, W. (2022). Analysis of flavonoid-related metabolites in different tissues and fruit developmental stages of blackberry based on metabolome analysis. *Food Research International*, *163*, Article 112313. <https://doi.org/10.1016/j.foodres.2022.112313>
- Xia, T., Xiong, Z., Sun, X., Chen, J., Wang, C., Chen, Y., & Zheng, D. (2023). Metabolomic profiles and health-promoting functions of Camellia drupifera mature-seeds were revealed relate to their geographical origins using comparative metabolomic analysis and network pharmacology approach. *Food Chemistry*, *426*, Article 136619. <https://doi.org/10.1016/j.foodchem.2023.136619>
- Zha, H., Cai, Y., Yin, Y., Wang, Z., Li, K., & Zhu, Z.-J. (2018). SWATHtoMRM: Development of High-Coverage Targeted Metabolomics Method Using SWATH Technology for Biomarker Discovery. *Analytical Chemistry*, *90*(6), 4062–4070. <https://doi.org/10.1021/acs.analchem.7b05318>
- Zhang, R., Zhu, X., Bai, H., & Ning, K. (2019). Network Pharmacology Databases for Traditional Chinese Medicine: Review and Assessment. *Frontiers in Pharmacology*, *10*. <https://doi.org/10.3389/fphar.2019.00123>
- Zhang, W., Sang, S., Peng, C., Li, G. Q., Ou, L., Feng, Z., ... Yao, M. (2022). Network Pharmacology and Transcriptomic Sequencing Analyses Reveal the Molecular Mechanism of Sanguisorba officinalis Against Colorectal Cancer. *Frontiers in Oncology*, *12*. <https://doi.org/10.3389/fonc.2022.807718>
- Zhang, Z.-M., Tong, X., Peng, Y., Ma, P., Zhang, M.-J., Lu, H.-M., ... Liang, Y.-Z. (2015). Multiscale peak detection in wavelet space. *Analyst*, *140*(23), 7955–7964. <https://doi.org/10.1039/c5an01816a>